

Supplemental Material for "Dynamical visualization of attractively interacting single vortices in type-II/1 superconducting Nb by magneto-optical imaging"

S. Ooi¹, M. Tachiki¹, T. Mochiku¹, H. Ito², T. Kubo^{2,3},
A. Kikuchi⁴, S. Arisawa⁴, K. Umemori^{2,3}

¹*International Center for Materials Nanoarchitectonics, National Institute for Materials Science, Sengen 1-2-1, Tsukuba 305-0047, Japan*

²*High Energy Accelerator Research Organization, 1-1 Oho, Tsukuba 305-0801, Japan*

³*SOKENDAI (The Graduate University for Advanced Studies), Hayama 240-0193, Japan*

⁴*Research Center for Energy and Environmental Materials (GREEN), National Institute for Materials Science, Sengen 1-2-1, Tsukuba 305-0047, Japan*

I. MOLECULAR DYNAMICS SIMULATION ON CLUSTERING VORTICES

As a demonstration to see how the vortices form clusters in the case of Eq. (A1) and (A2), we performed a two-dimensional MD simulation with COMSOL Multiphysics®[1] based on the force balance equations for each massless vortex $\sum_{j,j \neq i} \mathbf{F}_{i,j}^{v-v} = \eta_v \mathbf{v}_i$, where \mathbf{v}_i is the velocity of the i -th vortex and η_v is the viscous coefficient. In the present simulations, η_v is set to 10^{-6} dyn·s/cm², and the values of λ_L and κ are the same as in Appendix A. N is the number of vortices confined in a circular area of 30 μm diameter. An initial state where the vortices are almost uniformly separated is prepared using the repulsive vortex-vortex

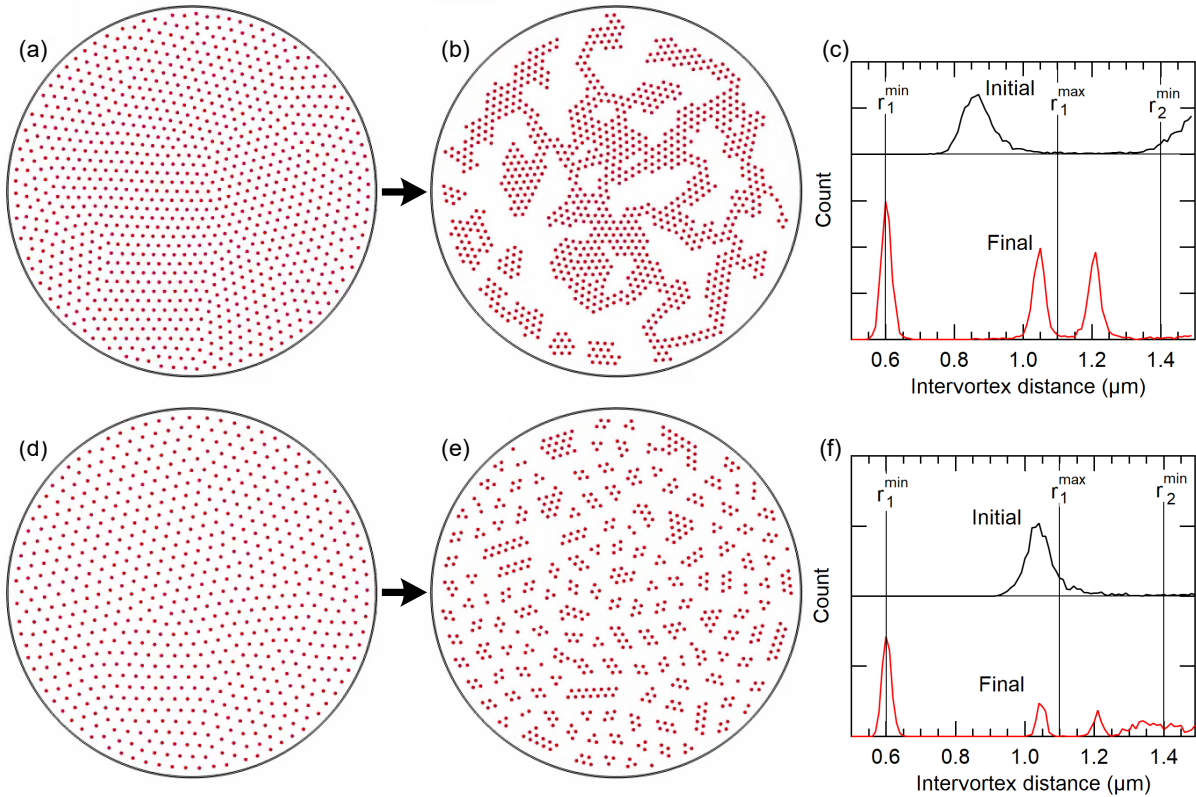


FIG. S1. Vortex configurations of (a) initial and (b) final states in the simulations for $N=1000$. (c) Histograms of the number of vortices as a function of intervortex distance for (a) and (b). (d,e,f) Configurations and histograms for $N=700$. The three peaks in the histogram of the final states correspond to the first, second and third nearest neighbors of the vortex lattice, from left to right. The temporal evolution of the clustering can be observed in the videos 'MD1_N1000.mp4' and 'MD2_N700.mp4' in the Supplemental Material.

interaction for the London limit of type-II superconductors. In the following, the positions r of the first and second local minima and the local maximum between them of the potential depicted in Fig. 6 are denoted as r_1^{\min} , r_2^{\min} , and r_1^{\max} , respectively.

The vortex configurations of the initial state and the final state after sufficient time elapsed are shown in Fig. S1(a,b) and (d,e) for $N=1000$ and 700 , respectively. The histograms of the number of vortices by intervortex distance are shown in Fig. S1(c) and (f). In both final states, the vortices form clusters or larger domains of hexagonal lattice with a lattice constant a_0 of $0.6 \mu\text{m}$, nearly the same value as r_1^{\min} . The size of the clusters tends to be larger for larger N , corresponding to larger B , which is consistent with our observations.

When N is sufficiently small, clusters formed by the interaction force from the first potential minimum do not appear. However, vortices can be aggregated by the force from the second potential minimum after a longer elapsed time as shown in Fig. S2, where a_0 of the initial state is larger than r_2^{\min} . It seems that this situation is rarely observed because the other forces, i.e. pinning force, driving force by the screening current, etc., exceed the second attractive interaction force in the actual experimental conditions.

II. VIDEOS OF MO OBSERVATIONS

In the Supplemental Material, Video1 to 3 are provided for Figs. 2-4 in the main text. In addition, Video4 to 6 are also provided for reference, obtained in three other fields of

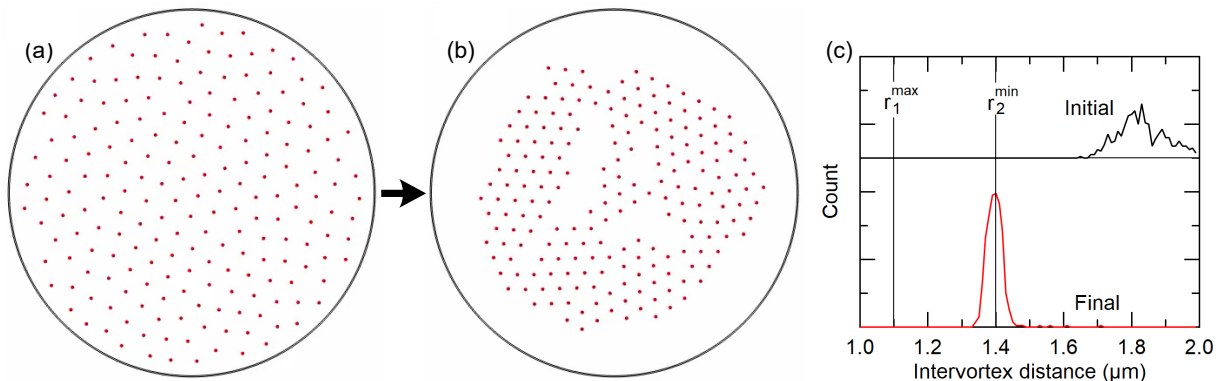


FIG. S2. Vortex configurations of (a) initial and (b) final states in the simulation for $N=200$. The corresponding video is 'MD3_N200.mp4' in the Supplemental Material. (c) Histograms of the number of vortices by intervortex distance for the initial and final states.

-4.3, 10.7, and -14.3 Oe, respectively. The images are taken during field cooling under the condition of an exposure time of 500 msec and no interval between successive images. The elapsed time from the first image is shown at the top left of the videos. For image processing, Fiji [2] is used for background subtraction, filtering, resizing, and AVI conversion, and MATLAB [3] is used for image registration.

Although we have used the eclipse PLD method to improve the quality of the MO films, the films still contain visible defects, probably precipitates or tiny droplets, which interfere with the vortex observation in the images. As can be seen, even after the image registration and the background subtraction, the processed images still show the traces of the defects.

REFERENCES

- [1] COMSOL Multiphysics® www.comsol.com. COMSOL AB, Stockholm, Sweden.
- [2] J. Schindelin, I. Arganda-Carreras, E. Frise, V. Kaynig, M. Longair, T. Pietzsch, S. Preibisch, C. Rueden, S. Saalfeld, B. Schmid, J.-Y. Tinevez, D. J. White, V. Hartenstein, K. Eliceiri, P. Tomancak, and A. Cardona, Fiji: an open-source platform for biological-image analysis, *Nature Methods* **9**, 676 (2012).
- [3] MATLAB version: 9.11.0 (R2021b), Natick, Massachusetts: The MathWorks Inc.; 2021.